OCEAN TARGET MONITORING WITH IMPROVED REVISIT TIME USING CONSTELLATIONS OF GNSS-R INSTRUMENTS

Alessio Di Simone [(1)], Hyuk Park [(2)], Daniele Riccio [(1)], Adriano Camps [(2)]

[(1)] Università di Napoli Federico II, Via Claudio 21, 80125, Naples, Italy
[(2)] Universitat Politècnica de Catalunya, Campus Nord, building D4, 08034, Barcelona, Spain

ABSTRACT

Ships and ice monitoring is of key importance in numerous applications, such as maritime traffic control, prevention of illegal activities, climate change studies, and maritime security. In this work, the feasibility of near real-time ocean target detection from a constellation of spaceborne Global Navigation Satellite System-Reflectometry (GNSS-R) images is demonstrated by addressing the two following points: 1) simulation of the revisit time allowed by constellations of GNSS-R instruments; 2) derivation and implementation of an ocean target detector aimed at identifying inhomogeneous features inside the delay-Doppler map. The revisit time is computed by simulating a realistic mission as a function of the constellation size and the number of receiving channels of the GNSS-R instrument. The proposed ocean target detection algorithm consists of four steps – pre-processing, pre-screening, selection, and geolocation – and is validated using actual U. K. TechDemoSat-1 data.

Index Terms— Global Navigation Satellite System-Reflectometry (GNSS-R), ocean target detection, maritime surveillance, sea state, constant false alarm rate (CFAR).

1. INTRODUCTION

The monitoring of inhomogeneous features on the sea surface, such as ice sheets and ships, impacts hydrological, biological, chemical and geological processes at and near the Earth' surface.

Ice sheet mapping plays a key role in numerous applications, such as climate changes analysis and maritime security. Despite their high accuracy, in-situ measurements only provide local information and a coverage limited to the Northern Hemisphere midlatitudes [1]. In order to address accurate ice sheet mapping at a global scale, spaceborne measurements from satellite constellations come into play.

Detection and monitoring of ships is important in maritime traffic control, illegal activities prevention, environment and pollution control, and naval warfare [2]. Despite the comprehensive information – name, speed, course, etc. – purchasable, the automatic identification system (AIS) protocol allows for sea traffic control within a limited area off the coastal line [2].

Remote sensing provides an unquestionable support in sea and ice monitoring, thanks to the global coverage. In particular, during the last three decades, synthetic aperture radar (SAR) and optical data have been extensively exploited in the sea target detection field [2-5], with an increased interest after the launch of recent missions, such as RADARSAT-2, COSMO-SkyMed, and the EU Copernicus system. Despite their high spatial resolution, SAR and optical satellites offer a temporal resolution, i.e., revisit time, on the order of days that affects the exploitation of such systems for near real-time sea monitoring. Indeed, it is noteworthy that a temporal resolution of the order of hours is required for ship detection [6]; the World Meteorological Organization indicates a revisit time of the order of hours for sea-ice cover concerning the Global Numerical Weather Prediction, climate monitoring and ocean applications [7].

Global Navigation Satellite System-Reflectometry (GNSS-R) is a recently remote sensing approach mainly exploited for sea state estimation [8], [9]. Due to its low cost, low power consumption, low size, and low weight, GNSS-R instruments can be launched in constellation formation at a relative low cost, fulfilling the temporal requirements for near real-time ship and ice monitoring as shown in the following section.

2. REVISIT TIME

In this section, the revisit time provided by constellations of satellites carrying GNSS-R payloads is analyzed. It depends upon numerous parameters concerning both the platform, the constellation and the surface roughness. Among them, the influence of the constellation size, satellite attitude and orbit inclination, number of receiving channels and GNSS transmitters tracked can be addressed in a deterministic framework by computing the orbital track of both transmitters and receivers. Other parameters, such as the Earth' surface roughness, influence the glistening zone size and the specular point position in a really complicated way; an accurate knowledge of the surface roughness up to the radar wavelength is required to determine the glistening zone size [10]. If such information is not available, a

stochastic approach can be followed to describe the surface height. Using this methodology, the revisit time turns into a spatial random process determined by the deterministic orbital parameters and the random specular point position and glistening zone size.

In this work, the revisit time is determined as a function of the constellation size and the number of receiving channels, leaving the influence of further parameters to future research activities. A realistic mission scenario has been defined to estimate the global revisit time. All the main current GNSS constellations, namely GPS, GLONASS, Galileo and BeiDou, are tracked. The Earth' surface is divided in 1°x1° cells, corresponding to a 120x120 km^2 cell at the Equator and a 120x40 km^2 cell at 70° N. For each point of the Earth' surface, (i.e., the 1°x1° cell) the revisit time is computed by averaging the time gaps between two consecutive passages of the specular point. For the specular point computation, the position of both GNSS transmitters and GNSS-R receivers have been taken into account and computed by means of mission simulation via the AGI Systems Tool Kit (STK®) software. Orbital and platform parameters – attitude, inclination, number of satellites, number of receiving channels, and GNSS systems tracked – are set according to Table I.

Fig. 1 shows the estimated global average revisit time as a function of the number of receiving channels for one (black line), eight (magenta line), sixteen (blue line), twenty-four (green line), and thirty-two (red line) GNSS-R satellites. As expected, the revisit time decreases with increasing number of satellites and receiving channels. Thus, in this simulated scenario, the minimum average revisit time (2 hours and 13 minutes) is reached with a constellation of 32 satellites tracking up to 16 GNSS transmitters, with an improvement of about 90% w.r.t. a single satellite tracking up to 16 transmitters and about 82% w.r.t. a 32-satellite constellation tracking only one transmitter. The possibility to track a larger number of glistening zones and specular reflection points justifies the decrease of the revisit time with increasing constellation size and number of receiving channels. However, the improvement of the revisit time with increasing tracking channels is bounded by the beamwidth of the zenith antenna that limits the number of GNSS transmitter accessible at a time. Consequently, only a limited set of tracking channels are operative at a time, and the addition of further channels does not contribute to further reduce the revisit time of the GNSS-R constellation. In the simulated scenario, a constant revisit time is achieved with more than 12 receiving channels.

3. PROPOSED SEA TARGET DETECTION ALGORITHM

In this section, a sea target detection algorithm for spaceborne GNSS-R Delay-Doppler map (DDM) is described. The proposed detector consists of four steps: pre-processing, pre-screening, selection, and geolocation.

3.1 Pre-processing

The pre-processing step aims at emphasizing the presence of a target within the Delay-Doppler (DD) domain and supporting the target extraction from GNSS-R observables. Concerning a DDM acquired over sea surface, it is noteworthy that each pixel consists of two contributions, namely thermal noise and sea clutter. If a target – sea ice sheet, ship – is present, a further contribution will appear in the corresponding DD cell. To enhance the presence of a target, the sea clutter term is estimated in the DD domain and suppressed in the pre-processing step, by evaluating the difference between the actual DDM and the simulated target-free one.

3.2 Pre-screening

In the pre-screening stage, the presence of targets is revealed as bright features in the difference map. Target candidates are then extracted by hard-thresholding of the difference map. The threshold is adaptively evaluated in order to account for clutter inhomogeneity and thermal noise so as to ensure a constant false alarm rate (CFAR).

3.3 Selection

In the selection stage, single-pixel targets are assumed to be false alarms caused by noise and, therefore, removed from the previous candidates map by means of a morphological operation. Small-to-medium islands, speckle noise can still cause false alarms.

3.4 Geolocation

In the geolocation stage, the geographic coordinates of the targets selected in the delay-Doppler domain are obtained. To this aim, the observation geometry should be reconstructed in the geographic reference frame, i.e., the positions and velocities of transmitter, receiver, and the specular reflection points are needed. Those data are available from the auxiliary of spaceborne GNSS-R mission, e.g., TDS-1 case from MERRByS website (http://www.merrbys.co.uk/). Once the observation geometry is reconstructed, the geographic coordinates of the target can be computed from its position in the delay-Doppler domain. Despite its simplicity, the geolocation step deserves a specific comment. In fact, a single position in delay-Doppler domain corresponds to two different geographic locations, due to the equi-Doppler and equi-range lines pattern in a bistatic configuration. It means that an ambiguity about the actual target location arises. To solve the ambiguity, a multilook approach can be used. A false location can be

filtered out from the DDMs acquired from multiple looks of the target. This multilook processing also increases the geolocation accuracy and the probability of detection.

4. EXPERIMENTAL RESULTS USING U. K. TDS-1 DATA

In this section, the proposed ocean target detection algorithm is tested with actual U. K. TDS-1 DDM. A probability of false alarms equal to 0.01 is considered in this case. The TDS-1 DDM used to test the algorithm is shown in Fig. 2a and was acquired on April 1st, 2015, at 00:19:49 UTC; the nominal specular point is at 47.47 N, 47.84 W. The pre-processing step (Fig. 2c) suppresses the sea clutter estimated in the simulated DDM in Fig. 2b. In the pre-screening stage, two sea targets are detected: a single-pixel target and an extended target. The isolated target is rejected as noise in the successive selection stage (Fig. 2e), while the extended target at about 1.34 C/A chips and 500 Hz in the DD domain is a sea ice sheet validated using the NSIDC sea ice extent data relevant to the same day [11].

TABLE I
ORBITAL AND PLATFORM PARAMETERS OF THE SIMULATED SCENARIO

Altitude [km]	500
Inclination [degree]	98°
Orbit type	Circular
Number of satellites	32
Number of parallel channels	16
GNSS systems tracked	GPS, Galileo, Glonass, BeiDou

5. ACKNOWLEDGMENTS

This project has received funding from the EU project "Operational Network of Individual Observation Nodes" (H2020-687490-ONION) of the Commission of European Communities and from "Técnicas avanzadas en teledetección aplicada usando señales GNSS y otras señales de oportunidad" AGORA (ESP2015-70014-C2-1-R) of the Spanish Ministry of Science and Competitiveness.

6. REFERENCES

[1] D. Robinson, K. Dewey and R. Heim, “Global Snow Cover Monitoring: An Update,” *Bulletin of the American Meteorological Society*, vol. 74, no. 9, pp. 1689-1696, 1993.

[2] S. Brusch, S. Lehner, T. Fritz, M. Soccorsi, A. Soloviev and B. van Schie, “Ship Surveillance With TerraSAR-X,” *IEEE Trans. Geosci. Remote Sens.*, vol. 49, no. 3, pp. 1092-1103, Mar. 2011.

[3] D. J. Crisp, “The state-of-the-art in ship detection in synthetic aperture radar imagery,” Intell., Surveillance and Reconnaissance Div., Inf. Sci. Lab., Def., Sci. Technol. Org., Edinburgh, S.A., Australia, May 2004, Res. Rep. DSTO-RR-0272.

[4] C. Zhu, H. Zhou, R. Wang and J. Guo, "A Novel Hierarchical Method of Ship Detection from Spaceborne Optical Image Based on Shape and Texture Features," *IEEE Trans. Geosci. Remote Sens.*, vol. 48, no. 9, pp. 3446-3456, Sept. 2010.

[5] G. Yang, B. Li, S. Ji, F. Gao and Q. Xu, "Ship Detection From Optical Satellite Images Based on Sea Surface Analysis," *IEEE Geosci. Remote Sens. Letters*, vol. 11, no. 3, pp. 641-645, Mar. 2014.

[6] P. Lombardo and M. Sciotti, "Segmentation-based technique for ship detection in SAR images," in *IEE Proceedings - Radar, Sonar and Navigation*, vol. 148, no. 3, pp. 147-159, Jun. 2001.

[7] Observing Systems Capability Analysis and Review Tool web site, Sea-ice cover requirements. https://www.wmo-sat.info/oscar/variables/view/135

[8] V. U. Zavorotny, S. Gleason, E. Cardellach and A. Camps, "Tutorial on Remote Sensing Using GNSS Bistatic Radar of Opportunity," *IEEE Geosci. Remote Sens. Mag.*, vol. 2, no. 4, pp. 8-45, Dec. 2014.

[9] E. Valencia, A. Camps, N. Rodriguez-Alvarez, H. Park and I. Ramos-Perez, "Using GNSS-R Imaging of the Ocean Surface for Oil Slick Detection," *IEEE J. Sel. Topics Appl. Earth Observ. in Remote Sens.*, vol. 6, no. 1, pp. 217-223, Feb. 2013.

[10] J. F. Marchan-Hernandez, A. Camps, N. Rodriguez-Alvarez, E. Valencia, X. Bosch-Lluis and I. Ramos-Perez, "An Efficient Algorithm to the Simulation of Delay–Doppler Maps of Reflected Global Navigation Satellite System Signals," *IEEE Trans. Geosci. Remote Sens.*, vol. 47, no. 8, pp. 2733-2740, Aug. 2009.

[11] J. Maslanik and J. Stroeve, "Near-Real-Time DMSP SSMIS Daily Polar Gridded Sea Ice Concentrations, Version 1. [nt_20150401_f17_nrt_n]," Boulder, Colorado USA. NASA National Snow and Ice Data Center Distributed Active Archive Center., 1999, updated daily. [Online]. Available: http://nsidc.org/data/nsidc-0081#. [Accessed 17 10 2016].

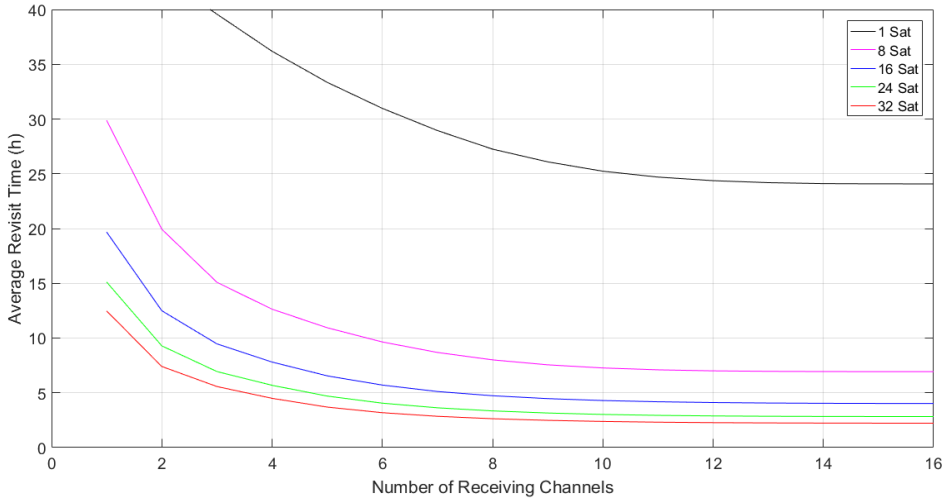

Fig. 1: Mean revisit time in hours vs. number of receiving channels considering one (black line), eight (magenta line), sixteen (blue line), twenty-four (green line), and thirty-two (red line) satellites. GPS, Galileo, Glonass, and BeiDou stations are tracked.

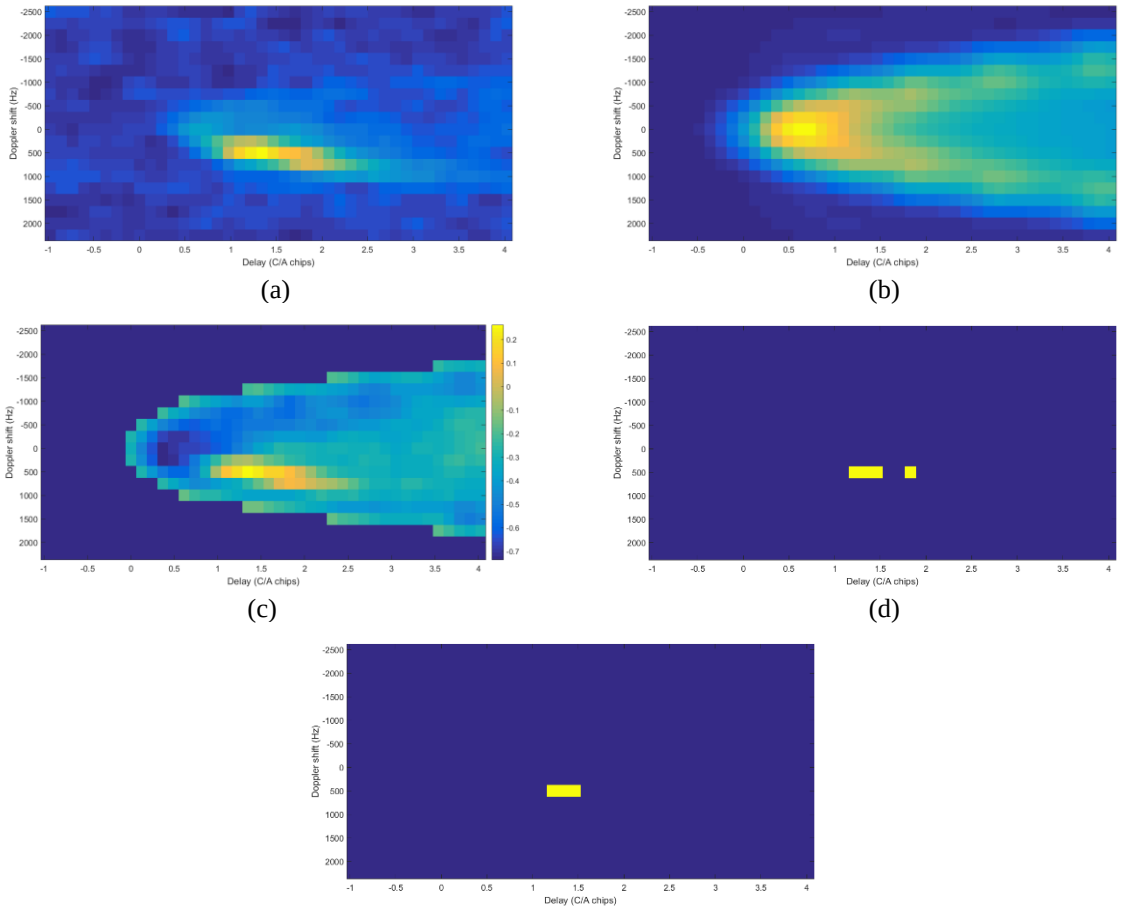

Fig. 2: (a) TDS-1 DDM acquired on April 1st, 2015 at 00:19:49 UTC. Nominal specular point at 47.47 N, 47.84 W. The visible bright feature is a sea ice sheet. (b) Simulated sea clutter contribution. (c) Difference map. (d) Pre-screening; (e) Selection. The detected target is a sea ice sheet validated using NSIDC data.